Impact of warmer climate periods on flood hazard in the European Alps

B. Wilhelm, W. Rapuc, B. Amann, F. S. Anselmetti, F. Arnaud, J. Blanchet, A. Brauer, M. Czymzik, C. Giguet-Covex, A. Gilli, et al.

ARTICLES
https://doi.org/10.1038/s41561-021-00878-y

nature geoscience

Impact of warmer climate periods on flood hazard in the European Alps

B. Wilhelm[1]✉, W. Rapuc[2], B. Amann[3,4], F. S. Anselmetti[5], F. Arnaud[2], J. Blanchet[1], A. Brauer[6], M. Czymzik[7], C. Giguet-Covex[2], A. Gilli[8], L. Glur[9], M. Grosjean[10], R. Irmler[11], M. Nicolle[12], P. Sabatier[2], T. Swierczynski[6] and S. B. Wirth[13,14]

Flooding is a pervasive natural hazard—costly in both human and economic terms—and climate change will probably exacerbate risks around the world. Mountainous areas, such as the densely populated European Alps, are of particular concern as topography and atmospheric conditions can result in large and sudden floods. In addition, the Alps are experiencing a high warming rate, which is probably leading to more heavy rainfall events. Here, we compile palaeoflood records to test the still uncertain impact these climatic trends might have on flood frequency and magnitude in the European Alps. We demonstrate that a warming of 0.5–1.2 °C, whether naturally or anthropogenically forced, led to a 25–50% decrease in the frequency of large (≥10 yr return period) floods. This decreasing trend is not conclusive in records covering less than 200 years but persistent in those ranging from 200 to 9,000 years. By contrast, extreme (>100 yr) floods may increase with a similar degree of warming in certain small alpine catchments impacted by local intensification of extreme rainfall. Our results show how long, continuous palaeoflood records can be used to disentangle complex climate–flooding relationships and assist in improving risk assessment and management at a regional scale.

Flooding is the most common type of climate-related disaster, resulting in annual losses estimated at US$50 billion and affecting 2.3 billion people over the period from 1994 to 2013[1]. Losses and casualties are likely to increase under a warming climate in response to the projected increases in heavy precipitation[2,3]. This scenario is very likely in mountainous regions, where the rate of warming is amplified[4,5] and may result in more precipitation extremes[3,6,7]. This change in precipitation extremes will also be accompanied by changes in mountain hydrological processes such as reduced snow depth, snow-cover duration or glacial extent[8]. Hence, the densely populated European Alps could become one of the hotspots of climate change-induced disasters in the coming decades. Thus, as a key matter for public concern, we aim to assess how flood hazards evolve under warmer climates.

Projections of flood hazard still encompass large uncertainties at the European scale and even larger at regional scales, which are the most relevant scales for stakeholders[9]. Recent work based on observations has revealed spatially consistent patterns of changes in flood hazard at the European scale. While an increase in the magnitude of the annual flood discharge has been observed in northwestern Europe, the magnitude tends to decrease in eastern and southern regions[10]. By contrast, a heterogeneous pattern of inconsistent trends has been found for the European Alps, and it remains unclear how flood discharges have evolved over recent decades[8,10–12]. The evolution of events larger than annual events is key for stakeholders as those events exhibit a greater potential to impact societies. However, the shortness of hydrometric records greatly limits our knowledge of the evolution of the intrinsically rare, most extreme events. Documenting changes in flood activity is even more complicated in small catchments[10,13,14]. Numerous small catchments occur in the complex Alpine orography but are rarely gauged, although they are considered the most sensitive to the projected increase in heavy rainfall[3,6,10]. Indeed, characteristics of flood-inducing rainfalls may differ with the catchment sizes[10,15]. Combined with the relative contribution of snow and glacier melt for the respective catchment topography and elevation, this results in various flood types in the European Alps[15],which, in turn, probably result in different flood trends as expected, for example, between the small and the most studied large catchments[10–15]. Therefore, our knowledge of the response of large and extreme floods to past, current and future warming is still limited in the European Alps, a place of exacerbated hydroclimate changes[8].

In this article, we analyse the most comprehensive dataset of long-term, continuous geology-based flood records from the European Alps. The dataset consists of 32 published (Fig. 1 and Extended Data Table 1)[16–37] and 1 unpublished (Extended Data Figs. 1 and 2 and Extended Data Table 2) record spanning up to 10,000 years. The continuous character of lake sediments guarantees the record continuity over time[38]. All 33 records provide information on past flood occurrences and 5 of them also include the flood magnitude. The dataset passed a screening procedure of hydrological, sedimentary and geochronological controls (Methods), resulting in

[1]Université Grenoble Alpes, CNRS, IRD, Grenoble INP, Institute for Geosciences and Environmental research (IGE), Grenoble, France. [2]Université Savoie Mont Blanc, CNRS UMR 5204, EDYTEM, Chambéry, France. [3]Renard Centre of Marine Geology, Ghent University, Ghent, Belgium. [4]UMR 7266 Littoral, Environnement et Sociétés (LIENSs), CNRS-Université de La Rochelle, La Rochelle, France. [5]Institute of Geological Sciences and Oeschger Centre for Climate Change Research, University of Bern, Bern, Switzerland. [6]GFZ German Research Centre for Geosciences, Potsdam, Germany. [7]Leibniz Institute for Baltic Sea Research Warnemünde (IOW), Rostock, Germany. [8]Geological Institute, ETH Zurich, Zurich, Switzerland. [9]Helvetia Swiss Insurance Company Ltd, St Gallen, Switzerland. [10]Oeschger Centre for Climate Change Research and Institute of Geography, University of Bern, Bern, Switzerland. [11]Institut für Geographie, Friedrich-Schiller Universität Jena, Jena, Germany. [12]Normandie Université, Unirouen, Unicaen, CNRS, M2C, Rouen, France. [13]Centre for Hydrogeology and Geothermics, University of Neuchâtel, Neuchâtel, Switzerland. [14]Present address: GEOTEST AG, Zollikofen, Switzerland. ✉e-mail: bruno.wilhelm@univ-grenoble-alpes.fr

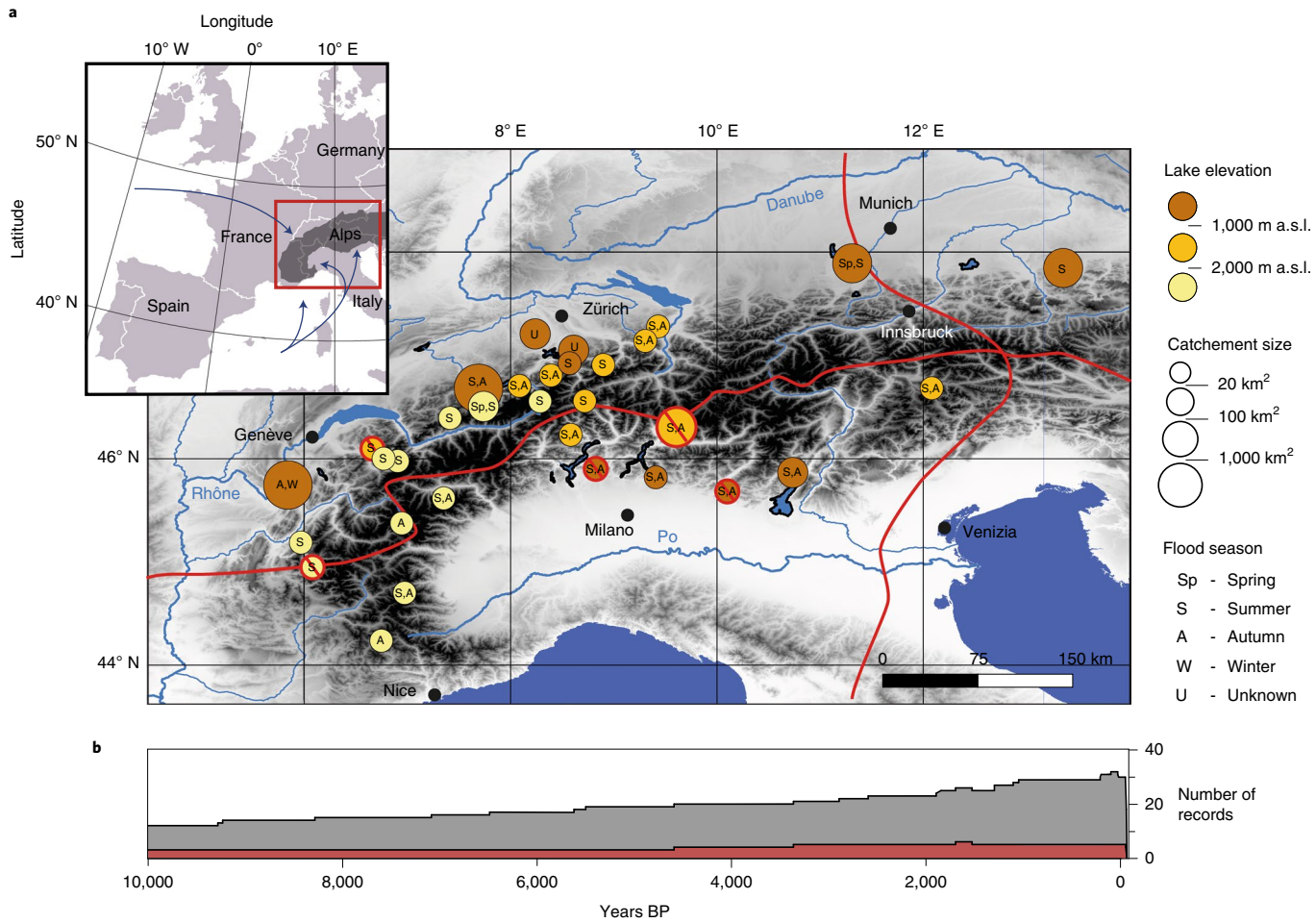

Fig. 1 | Spatiotemporal distribution of flood records from lake sediments available in the European Alps. a, Map showing the locations of flood records collected in this study. Points crossed out in red are records excluded from analyses. The red lines delimit the climate domains of the European Alps in relation to the relative proximity of the Atlantic Ocean, the Mediterranean Sea or the continental domain[4]. **b**, Temporal coverage of flood records. Those in red are excluded from analyses. Basemap (EU-DEM v.1.1) provided by Copernicus Land Monitoring Service, with funding by the European Union. a.s.l., above sea level.

a final selection of 27 records that continuously span the past 150 to 10,000 years, thereby documenting a total of 7,792 floods with a mean return period of 32 years (Extended Data Table 3). Documented catchments are distributed across the entire Alpine region, covering the Atlantic, Mediterranean and continental hydroclimate sectors[4]. Their surfaces range in size from 1 to 4,600 km^2, and their outlet elevation ranges from 198 to 2,620 m above sea level, thereby covering the whole diversity of Alpine flood types[15]. In line with the Alpine flood climatology[39], summer is the main season of recorded floods (Extended Data Table 1). To investigate the covariability between floods and temperature, temperature records from instrumental data and various proxies (chironomids, late wood density, tree ring width and water isotopes), all representative of the European Alps, are considered (Extended Data Table 4). Temperature is considered as a proxy for climate change, including changes in the atmospheric processes, and is therefore of relevance for assessing past and future changes in flood frequency[40].

To better understand the response of the flood occurrence to a warmer climate at various timescales, we analyse changes in their occurrence rates over three periods: the industrial era (IE, 1800–2000), the last millennium (LM, 950–1850) and a large part of the Holocene (9,000–1,000 years BP). Each period includes a pair of cooler and warmer subperiods that are all climatically well defined according to the literature (Methods). The level of cooling or warming between subperiods is here assessed as the mean change in temperature observed across all proxy-based reconstructions (Extended Data Table 5). The IE experienced a warming of 0.5 °C between the nineteenth (1800–1900) and twentieth (1900–2000) centuries, influenced largely by anthropogenic greenhouse gas emissions[41]. The LM includes the Medieval Climate Anomaly (MCA, 950–1250), which was 1 °C (±0.4) warmer than the Little Ice Age (LIA, 1450–1850)[42]. The Holocene includes the Holocene thermal maximum (HTM, 9,000–5,000 years BP), which was on average 1.2 °C (±0.4) warmer than the Neoglacial period (NP, 5,000–1,000 years BP)[43]. The Holocene and the LM periods, as defined here, do not extend to the IE; thus, they represent the natural climate variability[41,43]. When analysing flood–temperature relationships, each palaeoflood record is considered independently to investigate whether any changes in flood occurrence from cooler to warmer subperiods are spatially heterogeneous or regionally consistent, regardless of interrecords variability in terms of the flood timing, flood processes or catchment sensitivity.

Lower occurrence of large floods during warmer time intervals

First, analogous to modern projections that assess changes in climate variables between present and future warmer conditions[2,6,8], we determine the changes in the occurrence of large (≥10 yr) floods between past cooler and warmer subperiods. Our results reveal

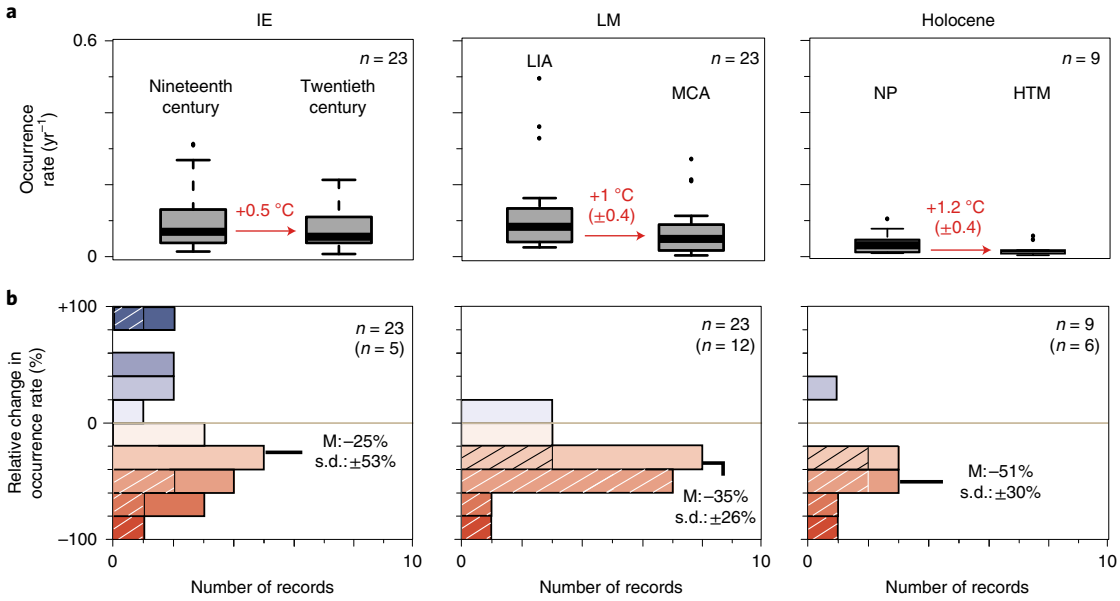

Fig. 2 | Changes in large-flood occurrence from cooler to warmer climates. a, Changes in the large-flood occurrence rate between the cooler and the warmer subperiods when considering all records. The occurrence rate is defined as the average number of flood events recorded per year at a given site during a subperiod. The changes in the temperature between the subperiods are assessed from Alpine temperature reconstructions (Methods and Extended Data Tables 4 and 5). In each plot, the bold centre line indicates the median, the box limits indicate the upper and lower quartiles, the whiskers indicate 1.5 × the interquartile range. **b**, Relative changes in the occurrence rate from the cooler to the warmer subperiods. The hatched areas highlight the number of records with significant changes among all records. *n*, total number of records considered in the analysis; (*n*), number of records with a significant change between subperiods; M, the median value.

significantly lower flood occurrence rates during the warmer subperiods at all timescales (Fig. 2a and Extended Data Table 6). We find a more pronounced decrease in flood occurrence from the IE to the LM and to the Holocene, with median values of −25% (standard deviation (s.d.): ±53%), −35% (s.d.: ±26%) and −51% (s.d.: ±30%), respectively. The number of palaeoflood records for which this trend is valid increases with the length of the period considered, with 68% of the records for the IE and up to 89% of the records for the Holocene (Fig. 2b). This pattern is spatially consistent at the Alpine scale except for the eastern Alps, where an increase in flood occurrence is observed under warmer conditions. This exceptional pattern is coherent with results from instrumental data[12,14] and climate projections[6]. This may result from the specific occurrence of extreme precipitation events lasting for several days due to the high moisture flux originating from the Adriatic Sea[12].

Decreasing trends in large-flood occurrence under warming conditions

Second, we analyse the occurrence trends of large floods during periods of warming or cooling. This approach follows trend analysis techniques using modern discharge data[10,11]. The trend analysis is performed for the three complete periods (over 200 years for the IE, 900 years for the LM and 8,000 years for the Holocene), which are all characterized by a significant warming (IE) or cooling (LM, Holocene) trend (Extended Data Table 7). The results reveal a regionally consistent, decreasing (increasing) trend in the occurrence of large floods under warming (cooling) climate (Fig. 3a–c). This trend is valid regardless of the length of the period considered, from hundreds to thousands of years. The same analysis is then applied over shorter time windows, ranging from the past 50 to the past 150 years (Fig. 3d–f), to identify the shortest period required for the trend pattern to be identified. The number of records with significant trends is small (33%) for the shortest and most recent period (1950–2000), which corresponds to the most common time length of gauged data. The few significant trends mirror previous findings[11], with a heterogeneous pattern over the Alps characterized by increasing flood trends in the northwestern region and decreasing trends in the southeastern region. The number of records with significant trends progressively increases when considering longer time series. Significant trends outnumber insignificant trends during periods longer than 150 years (1850–2000). In addition, the decreasing (increasing) trend under warming (cooling) becomes consistent in direction and space as well as persists during all periods longer than 150 years, a duration poorly or not covered by gauged data. Hence, whereas flood-rich periods have already been recognized to occur mostly during decadal cooler periods in the European Alps[20,30] and surrounding areas[40,44], we show here that the increase in large-flood occurrence under cooling in the Alps is regionally consistent and persistent in time as soon as records are longer than 200 years.

Climate and land-cover changes are usually considered the main drivers of changes in the flood frequency and magnitude[13]. Given the studied timescales, the changes in land cover correspond mostly with changes in the ratio between forest and grassland areas. Such changes differ in time and space between catchments according to their location, elevation and human activities. Our regionally consistent flood pattern suggests that the influence of land-cover changes is minimal as it would result in a spatially heterogeneous flood pattern. Moreover, the high-elevation sites exhibit the same flood pattern as that recorded at low or medium elevations, while high-elevation vegetation cover (mainly bare land and Alpine meadow) changes very little over time. Therefore, we interpret the observed flood pattern as driven by the hydroclimate variability, such as snow melt, soil moisture and precipitation[10,12]. In the Alps, the role of snow melt is recognized as being limited to the generation of a small fraction of flood events[12]. In addition, instrumental data reveal site-specific trends with both increasing and decreasing occurrences of rain-on-snow events related to the warming over

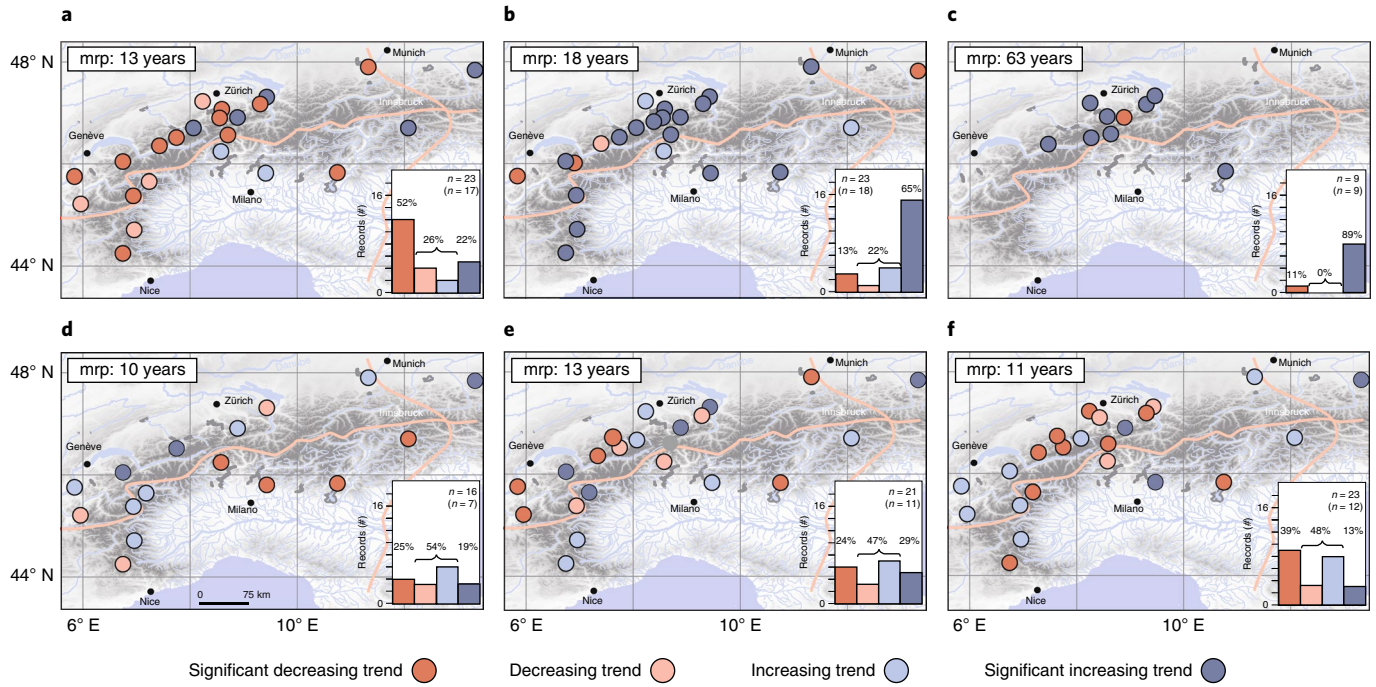

Fig. 3 | Trends in the occurrence of large floods during periods with warming or cooling trends. a, IE, significant warming trend. **b**, LM, significant cooling trend. **c**, Holocene, significant cooling trend. **d**, 1950–2000, significant warming trend. **e**, 1900–2000, significant warming trend. **f**, 1850–2000, significant warming trend. mrp, mean return period (the number of recorded flood events divided by the considered time length); *n*, total number of records considered in the trend analysis; (*n*), number of records with a significant trend (a significance level of $\alpha = 0.1$ is considered). Basemap (EU-DEM v.1.1) provided by Copernicus Land Monitoring Service, with funding by the European Union.

the past decades[12,45,46]. Therefore, the changes in snow cover and related rain-on-snow events do not seem to be the best candidates to explain our observed regionally consistent flood pattern. By contrast, short-rainfall events associated with synoptic weather types are recognized as the main Alpine hydroclimate flood drivers[12,39]. Higher precipitation has been documented for each of the cooler subperiods, at the annual scale from changes in lake level and pollen assemblages[46,47] as well as during the warm season from varve thickness[30]. Lower temperatures could additionally induce a lower evapotranspiration, resulting in soil moisture increasing and promoting the generation of floods[10,14]. Such conditions during cooler periods have been explained by changes in the prevailing westerly winds and associated storm tracks, related to their intensification[48,49], their zonal shift[20,50,51] or both[52,53]. Therefore, the changes in both the mean and heavy precipitation linked to these regional climate-related atmospheric processes are the most likely candidates to explain the observed decrease (increase) in large floods during warmer (cooler) periods.

From large- to extreme-flood occurrence during warmer climate intervals

A challenge in flood risk assessment is the estimation and evolution of the 100 yr flood discharge, which is often used as a key design criterion. The 100 yr flood discharges are rarely observed instrumentally due to the short period of gauged data. Thereby, trends in 100 yr floods rely either on statistically estimated discharges[14] or on the assumption that annual floods and more extreme floods are usually closely correlated[10]. Both approaches encompass intrinsic uncertainties that are, however, difficult to assess due to the lack of long-term observations. Here, our dataset contains five continuous series of extreme (≥100 yr) flood occurrence, allowing to explore with field evidence the stability of trends when considering distinct return periods. Similarly to our first analysis, we count in each of the five records the number of occurrences of large and extreme floods during the cool LIA and the warm MCA. Only subperiods of the LM are considered in the analysis because the IE is too short to offer a sufficient number of extreme floods for analysis, and records with flood magnitude information do not extend to the Holocene (Extended Data Table 1). For large floods, all records show fewer occurrences during the warmer subperiod (Fig. 4a), consistent with our previous results (Fig. 2). However, trends in extreme floods are more contrasted, with more events during the LIA subperiod in three of the records (purple dots, Fig. 4b) and during the MCA subperiod in the other two records (green dots, Fig. 4b). Therefore, our results suggest that the trends in large floods cannot be systematically extrapolated to obtain the trends in extreme floods. This calls for caution when performing such an extrapolation in modern flood hydrology. Our results are, however, based on a small sample of field evidence, which limits their robustness. This should encourage future work in palaeoflood hydrology to systematically document, whenever possible, the magnitude of past floods. This work appears particularly valuable for some small catchments that may be affected by an increasing flood hazard[2], as those for which we observe an increasing occurrence of extreme floods during the warmer subperiod (green dots, Fig. 4b). Indeed, small catchments are places where floods are triggered mostly by local, short-duration and high-intensity convective storms[10,39], expected to be highly intensified at local scales under a warmer climate[2,6,10].

This study highlights the great value of palaeoflood data to detect and better understand regional trends in large and extreme floods[54]. Our palaeoflood dataset reveals robust trends that are regionally consistent and persistent regardless of the time window considered and the respective climate forcing. Although we advise care in extrapolating these findings to the future, especially in regard to climate scenarios with temperature levels higher than those during the warmest periods in our reconstructions[8], our dataset offers a unique

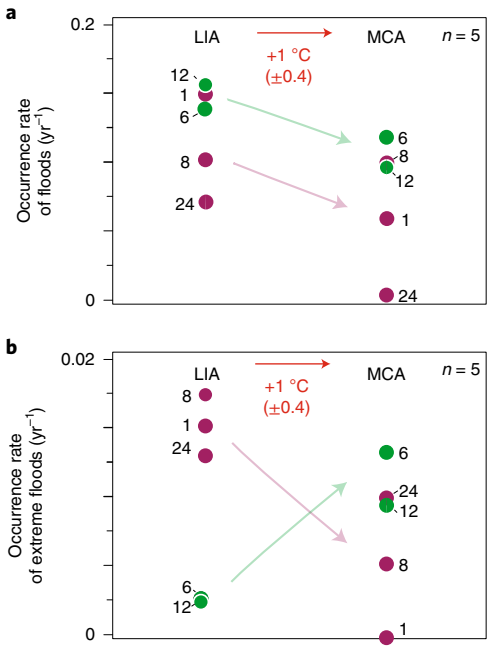

Fig. 4 | Changes in flood occurrence between the cool LIA and the warm MCA for the five records documenting flood magnitude. a, Changes in the occurrence rate of large floods. **b**, Changes in the occurrence rate of extreme floods. The numbers (1, 6, 8, 12 and 24) refer to the site numbers in Extended Data Tables 1 and 2. The records showing higher occurrence rates of extreme floods during the cooler (warmer) subperiod are marked in purple (green).

opportunity to test the flood modelling tools commonly applied for projections in a much wider range of climate variability than the one observed over the past decades[55]. This avenue is expected to greatly help improve our understanding of regional temperature–flood linkages under past and future climate conditions and, thereby, should ultimately lead to better flood hazard projections for more relevant flood risk management.

Online content

Any methods, additional references, Nature Research reporting summaries, source data, extended data, supplementary information, acknowledgements, peer review information; details of author contributions and competing interests; and statements of data and code availability are available at https://doi.org/10.1038/s41561-021-00878-y.

Received: 25 August 2020; Accepted: 18 November 2021;
Published online: 27 January 2022

References

1. Center for Research on the Epidemiology of Disasters (UNISDR). The human cost of natural disasters: A global perspective, 58 pp. Retrieved from http://cred.be/sites/default/files/The_Human_Cost_of_Natural_Disasters_CRED.pdf (CRED, 2015)
2. Dottori, F. et al. Increased human and economic losses from river flooding with anthropogenic warming. *Nat. Clim. Change* **8**, 781–786 (2018).
3. Fowler, H. J. et al. Anthropogenic intensification of short-duration rainfall extremes. *Nat. Rev. Earth Environ.* **2**, 107–122 (2021).
4. Auer, I. et al. HISTALP—historical instrumental climatological surface time series of the Greater Alpine Region. *Int. J. Climatol.* **27**, 17–46 (2007).
5. Pepin, N. et al. Elevation-dependent warming in mountain regions of the world. *Nat. Clim. Change* **5**, 424–430 (2015).
6. Giorgi, F. et al. Enhanced summer convective rainfall at Alpine high elevations in response to climate warming. *Nat. Geosci.* **9**, 584–589 (2016).
7. Ménégoz, M. et al. Contrasting seasonal changes in total and intense precipitation in the European Alps from 1903 to 2010. *Hydrol. Earth Sci. Syst.* **24**, 5355–5377 (2020).
8. IPCC: Summary for Policymakers. In *IPCC Special Report on the Ocean and Cryosphere in a Changing Climate* (eds Pörtner, H.-O. et al.) (IPCC, 2019).
9. Kundzewicz, Z. W. et al. Differences in flood hazard projections in Europe—their causes and consequences for decision-making. *Hydrol. Sci. J.* **62**, 1–14 (2016).
10. Blöschl, G. et al. Changing climate both increases and decreases European river floods. *Nature* **573**, 108–111 (2019).
11. Mangini, W. et al. Detection of trends in magnitude and frequency of flood peaks across Europe. *Hydrol. Sci. J.* **63**, 493–512 (2018).
12. Hundecha, Y., Parajka, J. & Viglione, A. Assessment of past flood changes across Europe based on flood-generating processes. *Hydrol. Sci. J.* **65**, 1830–1847 (2020).
13. Blöschl, G. et al. Increasing river floods: fiction or reality? *WIREs Water* **2**, 329–344 (2015).
14. Bertola, M., Viglione, A., Lun, D., Hall, J. & Blöschl, G. Flood trends in Europe: are changes in small and big floods different? *Hydrol. Earth Syst. Sci.* **24**, 1805–1822 (2020).
15. Tarasova, L. et al. Causative classification of flood events. *WIREs Water* **6**, e1353 (2019).
16. Wilhelm, B. et al. 1400 years of extreme precipitation patterns over the Mediterranean French Alps and possible forcing mechanisms. *Quat. Res.* **78**, 1–12 (2012).
17. Wirth, S. B., Glur, L., Gilli, A. & Anselmetti, F. S. Holocene flood frequency across the Central Alps—solar forcing and evidence for variations in North Atlantic atmospheric circulation. *Quat. Sci. Rev.* **80**, 112–128 (2013).
18. Czymzik, M. et al. Orbital and solar forcing of shifts in mid- to late Holocene flood intensity from varved sediments of pre-alpine Lake Ammersee (southern Germany). *Quat. Sci. Rev.* **61**, 96–110 (2013).
19. Giguet-Covex, C. et al. Frequency and intensity of high-altitude floods over the last 3.5 ka in NW European Alps. *Quat. Res.* **77**, 12–22 (2012).
20. Glur, L. et al. Frequent floods in the European Alps coincide with cooler periods of the past 2500 years. *Sci. Rep.* **3**, 2770 (2013).
21. Wilhelm, B. et al. Palaeoflood activity and climatic changes over the last 1400 years from lake sediments of the NW European Alps. *J. Quat. Sci.* **28**, 189–199 (2013).
22. Wilhelm, B. et al. Does global warming favour the occurrence of extreme floods in European Alps? First evidences from a NW Alps proglacial lake sediment record. *Clim. Change* **113**, 563–581 (2012).
23. Evin, G., Wilhelm, B. & Jenny, J. P. Flood hazard assessment of the Rhône River revisited with reconstructed discharges from lake sediments. *Glob. Planet. Change* **172**, 114–123 (2019).
24. Wirth, S. B. et al. Combining sedimentological, trace metal (Mn, Mo) and molecular evidence for reconstructing past water-column redox conditions: the example of meromictic Lake Cadagno (Swiss Alps). *Geochim. Cosmochim. Acta* **120**, 220–238 (2013).
25. Irmler, R., Daut, G. & Mäusbacher, R. A debris flow calendar derived from sediments of Lake Lago di Braies (N. Italy). *Geomorphology* **77**, 69–78 (2006).
26. Wilhelm, B., Vogel, H., Crouzet, C., Etienne, D. & Anselmetti, F. S. Frequency and intensity of palaeofloods at the interface of Atlantic and Mediterranean climate domains. *Climate* **12**, 299–316 (2016).
27. Wilhelm, B., Vogel, H. & Anselmetti, F. S. A multi-centennial record of past floods and earthquakes in Valle d'Aosta, Mediterranean Italian Alps. *Nat. Hazards Earth Syst. Sci.* **17**, 613–625 (2017).
28. Wirth, S. B. et al. A 2000-year long seasonal record of floods in the southern European Alps. *Geophys. Res. Lett.* **40**, 4025–4029 (2013).
29. Swierczynski, T. et al. Mid- to late Holocene flood frequency changes in the northeastern Alps as recorded in varved sediments of Lake Mondsee (Upper Austria). *Quarternary Sci. Rev.* **80**, 78–90 (2013).
30. Amann, B., Szidat, S. & Grosjean, M. A millennial-long record of warm season precipitation and flood frequency for the North-western Alps inferred from varved lake sediments: implications for the future. *Quat. Sci. Rev.* **115**, 89–100 (2015).
31. Sabatier, P. et al. 6-kyr record of flood frequency and intensity in the western Mediterranean Alps—interplay of solar and temperature forcing. *Quat. Sci. Rev.* **170**, 121–135 (2017).
32. Wirth, S. B., Girardclos, S., Rellstab, C. & Anselmetti, F. S. The sedimentary response to a pioneer geo-engineering project: tracking the Kander River deviation in the sediments of Lake Thun (Switzerland). *Sedimentology* **58**, 1737–1761 (2011).
33. Lauterbach, S. et al. DecLakes participants. A sedimentary record of Holocene surface runoff events and earthquake activity from Lake Iseo (Southern Alps, Italy). *Holocene* **22**, 749–760 (2012).
34. Rapuc, W. et al. Holocene-long record of flood frequency in Southern Alps (Lake Iseo, Italy) under human and climate forcing. *Glob. Planet. Change* **175**, 160–172 (2019).

35. Stewart, M., Grosjean, M., Kuglitsch, F. G., Nussbaumer, S. U. & von Gunten, L. Reconstructions of late Holocene palaeofloods and glacier length changes in the Upper Engadine, Switzerland (ca. 1450 BC–AD 420). *Palaeogeogr. Palaeoclimatol. Palaeoecol.* **311**, 215–123 (2011).
36. Bajard, M. et al. Pastoralism increased vulnerability of a subalpine catchment to flood hazard through changing soil properties. *Palaeogeogr. Palaeoclimatol. Palaeoecol.* **538**, 109462 (2019).
37. Fouinat, L. et al. Relationship between glacial activity and flood frequency in proglacial Lake Muzelle. *Quat. Res.* **87**, 407–422 (2017).
38. Wilhelm, B. et al. Interpreting historical, botanical, and geological evidence to aid preparations for future floods. *WIREs Water* **6**, e1318 (2018).
39. Parajka, J. et al. Seasonal characteristics of flood regimes across the Alpine–Carpathian range. *J. Hydrol.* **394**, 78–89 (2010).
40. Blöschl et al. Current European flood-rich period exceptional compared with past 500 years. *Nature* **583**, 560–566 (2020).
41. Schurer, A. P. et al. Small influence of solar variability on climate over the past millennium. *Nat. Geosci.* **7**, 104–108 (2014).
42. Jones, P. D., Osborn, T. J. & Briffa, K. R. The evolution of climate over the last millennium. *Science* **292**, 662–666 (2001).
43. Renssen, H. et al. The spatial and temporal complexity of the Holocene thermal maximum. *Nat. Geosci.* **2**, 411–414 (2009).
44. Mudelsee, M. et al. No upward trends in the occurrence of extreme floods in central Europe. *Nature* **425**, 166–169 (2003).
45. Beniston, M. & Stoffel, M. Rain-on-snow events, floods and climate change in the Alps: events may increase with warming up to 4 °C and decrease thereafter. *Sci. Total Environ.* **571**, 228–236 (2016).
46. Moran-Tejeda, E., Lopez-Moreno, J. I., Stoffel, M. & Beniston, M. Rain-on-snow events in Switzerland: recent observations and projections for the 21st century. *Clim. Res.* **71**, 111–125 (2016).
47. Magny, M., Bégeot, C., Guiot, J. & Peyron, O. Contrasting patterns of hydrological changes in Europe in response to Holocene climate cooling phases. *Quat. Sci. Rev.* **22**, 1589–1596 (2003).
48. Magny, M. et al. North–south palaeohydrological contrasts in the central Mediterranean during the Holocene: tentative synthesis and working hypotheses. *Climate* **9**, 2043–2071 (2013).
49. Goosse, H., Guiot, J., Mann, M. E., Dubinkina, S. & Sallaz-Damaz, Y. The medieval climate anomaly in Europe: comparison of the summer and annual mean signals in two reconstructions and in simulations with data assimilation. *Glob. Planet. Change* **84-85**, 35–47 (2012).
50. Yin, J. H. A consistent poleward shift of the storm tracks in simulations of 21st century climate. *Geophys. Res. Lett.* **32**, L18701 (2005).
51. Shi, X. & Durran, D. The response of orographic precipitation over idealized midlatitude mountains due to global increases in CO_2. *J. Climatol.* **27**, 3938–3956 (2014).
52. Bengtsson, L. & Hodges, K. I. Storm tracks and climate change. *J. Clim.* **19**, 3518–3543 (2006).
53. Raible, C. C., Yoshimori, M., Stocker, T. F. & Casty, C. Extreme midlatitude cyclones and their implications for precipitation and wind speed extremes in simulations of the Maunder Minimum versus present day conditions. *Clim. Dyn.* **28**, 409–423 (2007).
54. St. George, S., Hefner, A. M. & Avila, J. Paleofloods stage a comeback. *Nat. Geosci.* **13**, 766–768 (2020).
55. Harrison, S. P. et al. Evaluation of CMIP5 palaeo-simulations to improve climate projections. *Nat. Clim. Change* **5**, 735–743 (2015).

Methods

Datasets. Flood data. We systematically searched the scientific literature for flood records from lake sediment sequences, assisted by the interactive, online metadatabase of the Floods Working Group of the Past Global Changes structure. Only flood records from lake sediments were considered since they are the only archives that guarantee the record continuity over long periods[38]. We selected all records fulfilling the following criteria:

(1) Signal requirements: all records must contain dates of past flood deposits. Information on the past flood magnitude is not mandatory. The flood deposit thickness is systematically provided, but it was considered only when validated in the original publication as a proxy of the magnitude.
(2) Geographical requirements: all records must be located in the European Alps and its forelands, bounded by 5.5°–13.5° E and 43.5°–48° N.
(3) Publication requirements: we employed only records that were published in the scientific, peer-reviewed literature and thus validated by the community. The only original data are those presented in Extended Data, which aims to extend the published Lake Bourget record[23,56] to the LM following the method deployed by Jenny et al.[56]. In line with this study, a new set of cores has been sampled in 2017, in which flood layers have been identified and dated combining historical floods and three radiocarbon samples calibrated using the IntCal13 calibration curve[57] (Extended Data Fig. 1 and Table 2). The age–depth model has been processed using the software package 'clam'[58] with R software[59] (Extended Data Fig. 1). The evaluation performed with independent series[56,60] supports the reconstruction of the Rhône River floods over the LM (Extended Data Fig. 2).
(4) Temporal coverage: all palaeoflood records must continuously cover at least one period of interest: the past 150 years (1850–2000), the IE, the LM or the Holocene.

The database consists of flood occurrence dates over the past 150 to 10,000 years at 33 locations and includes proxies of the flood magnitude (the deposit thickness, spatial extent, grain size) at 5 of these 33 locations. The record density is globally high but rather uneven with most records in the western and central Alps (France, Switzerland and Italy) and a few records in the eastern part (Germany, Austria and Slovenia; Fig. 1 and Extended Data Table 1). Before starting the analysis, the dataset was further screened to exclude all records that did not fulfil the following hydrological, sedimentological and geochronological requirements.

For hydrological screening, any records from catchments that were known or identified to have experienced notable human modification (such as reservoirs) that could affect changes in the flood discharges and in-lake recording were excluded.

In terms of sedimentological screening, the hydroclimatic signal of flood records might be disturbed by changes in the erosion processes within the catchment owing to geomorphological (for example, large landslides, glaciers) or anthropogenic (for example, grazing, agriculture) impacts. Any records affected by such disturbances according to the original publications were also excluded. Local and/or isolated effects over time due to human or geomorphological activities could not be fully excluded from the records. This study was, however, focused on consistent flood change patterns at the regional and long-term scales.

For geochronological screening, we verified that the age–depth models of all records were constrained by at least two dating points over the past two centuries and by three dating points regarding the LM and the Holocene. For the two latter periods, at least one dating point (D1) should occur within the period of interest, and the remaining two should be close to the start (D2) and end (D3) dates of the period of interest. D2 can be located between the start date and the top of the core. The number of years between D3 and the end date should be less than 700 and 1,500 for the LM and the Holocene, respectively. The dating points included the tops of cores (the year of collection), ^{137}Cs chronomarkers, ^{210}Pb chronologies, historical events, palaeomagnetic features and radiocarbon dates, except for those performed on bulk sediments. Varved records were exempted from this procedure since they inherently benefit from an annual dating.

These hydrological, sedimentological and geochronological screenings resulted in a final set of 27 (out of the 33 available) records without a major change in the initial data density. The included lake records are characterized by a mean catchment area of 347 km^2 (a minimum of 1 and a maximum of 4,600) and a mean elevation of 1,486 m (a minimum of 198 and a maximum of 2,620) above sea level. The main seasonality of the recorded floods is from summer to autumn (Fig. 1 and Extended Data Table 1), which corresponds with the main observed flood seasons[18], and the mean return periods of these events are 14, 18 and 63 years for the past two centuries, the LM and the Holocene, respectively (Extended Data Table 3). Given the wide range of environmental and geographical settings of the 27 catchments, all types of Alpine floods are covered, namely, flash, short-rain, long-rain, snow-melt and rain-on-snow floods[15]. Subsets were finally defined for the analyses of the different periods of interest on the basis of their temporal coverage (Extended Data Table 3).

Temperature data: we systematically screened the scientific literature for Alpine temperature records covering the three periods of interest, regardless of the nature of the archive and/or proxy. We applied the same geographical, temporal and publication requirements as for the palaeoflood record selection (Extended Data Table 4).

The Holocene temperature record from the Milandre Cave, Switzerland[61], is not included because it reflects the mean annual temperature and not the summer flood season of the Holocene records. These datasets are used (1) to assess the regional changes in temperature between the cool and warm subperiods during the three periods of interest (Extended Data Table 5) and (2) to test the presence and significance of the warming trends during each of the three periods (Extended Data Table 7). The choice of the three study periods was guided by the trade-off between the record length of the available data (Fig. 1b and Extended Data Table 1) and the coverage of warmer versus cooler subperiods: (1) suitably documented in the scientific literature, (2) of similar time lengths, enabling a consistent comparison and (3) occurring under various natural and anthropogenic forcings. This resulted in the selection of three periods:

(1) The IE[41] records recent warming controlled mainly by anthropogenic increases in greenhouse gases. This period is documented in 23 of the 27 records. The subperiods are defined by using the Intergovernmental Panel on Climate Change upper time boundary of the 'preindustrial' baseline in 1900[41]. The IE has been divided into two equally long subperiods: the nineteenth century and the 0.5 °C warmer twentieth century.
(2) The LM[42,47] records the multicentennial warmer and cooler subperiods of the MCA and the LIA[62], respectively. The LIA is very well known for the large glacier advances in the Alps[63]. The difference in temperature between these two subperiods is $+1 \pm 0.4$ °C. This millennial period is also documented in a majority of records (23 out of the 27 records).
(3) The Holocene records the millennial-long warmer and cooler subperiods of the HTM (10,000–5,000 years BP) and the NP (5,000–0 years BP), respectively[49]. The start and end dates of these periods are slightly adapted by considering 9,000 years BP as the start date of the HTM and 1,000 years BP as the end date of the NP. Selecting this later HTM start date allows increasing the number of palaeoflood records from 7 to 9 (in the 27 records) (Table 1), and selecting the earlier NP end date limits the overlap with the LM, constraining the reuse of the same data for the independent analyses. In addition, these adaptations allow studying Holocene subperiods of equal time lengths. The difference in temperature between the two subperiods is $+1.2 \pm 0.4$ °C.

Data analyses. First, we assess the changes in flood occurrence between the cooler and the warmer subperiods of each period of interest (IE, LM and H). The flood occurrence is assessed through the occurrence rate, which is the average number of flood events recorded per year at a given site during a subperiod. This aims to obtain comparable results for all subperiods, regardless of their time lengths. A direct comparison of the occurrence rates is, however, possible only for pairs of subperiods of the same period since the datasets differ between periods. We apply the two-proportion z test at a confidence level of 95%[64], testing the null hypothesis that the proportions of flood in the two subperiods are equal against the alternative hypothesis that the proportion of flood is greater in the warmer subperiod (Extended Data Table 6). The relative change in the occurrence rate between pairs of subperiods is then calculated for each single record by systematically considering the cool period as the reference period. Hence, the relative change corresponds with the change in occurrence rates from the cooler to the warmer subperiods for each record (Fig. 2b).

In the second data analysis, we assess trends in flood occurrence, and whether they are significant, during periods exhibiting significant warming or cooling according to the non-parametric, modified Mann–Kendall test, taking into account the serial autocorrelation[65] (Extended Data Tables 6 and 7), that is, over the past 50 (1950–2000), 100 (1900–2000), 150 (1850–2000) and 200 (1800–2000) years as well as during the LM and a large part of the Holocene. The trends in flood occurrence during these periods are then detected following the method of Mangini et al.[11] by estimating a Poisson regression model with years as covariate (generalized linear regression model) and testing the trend significance with a chi-squared test. A trend is considered significant when the significance level α is smaller than 0.1 (Extended Data Table 6).

Data availability

The authors declare that the palaeoflood data supporting the findings of this study (Extended Data Table 1) are available in the NOAA database at the following address: https://www.ncei.noaa.gov/access/paleo-search/study/34712. The temperature data from Extended Data Table 4 are all available in the NOAA or PANGEA repositories.

References

56. Jenny, J. P. et al. A 4D sedimentological approach to reconstructing the flood frequency and intensity of the Rhône River (Lake Bourget, NW European Alps). *J. Paleolimnol.* **51**, 469–483 (2014).
57. Reimer, P. J. et al. IntCal13 and Marine13 radiocarbon age calibration curves 0–50,000 years cal BP. *Radiocarbon* **55**, 1869–1887 (2013).
58. Blaauw, M. Methods and code for 'classical' age-modelling of radiocarbon sequences. *Quat. Geochronol.* **5**, 512e518 (2010).

59. R Development Core Team *R: a Language and Environment for Statistical Computing* (R Foundation for Statistical Computing, 2011); http://www.R-project.org/
60. Arnaud, F. et al. Erosion under climate and human pressures: an alpine lake sediment perspective. *Quat. Sci. Rev.* **152**, 1–18 (2016).
61. Affolter, S. et al. Central Europe temperature constrained by speleothem fluid inclusion water isotopes over the past 14,000 years. *Sci. Adv.* **5**, eeav3809 (2019).
62. Masson-Delmotte, V. et al. in *Climate Change 2013: The Physical Science Basis* (eds Stocker, T. F. et al.) Ch. 5 (Cambridge Univ. Press, 2013).
63. Holzhauser, H., Magny, M. & Zumbühl, H. J. Glacier and lake-level variations in west-central Europe over the last 3500 years. *Holocene* **15**, 789–801 (2005).
64. Newcombe, R. G. Interval estimation for the difference between independent proportions: comparison of eleven methods. *Stat. Med.* **17**, 873–890 (1998).
65. Hamed, K. H. & Ramachandra, R. A modified Mann–Kendall trend test for autocorrelated data. *J. Hydrol.* **204**, 182–196 (1998).

Acknowledgements

The data collection and the study design have been facilitated by the PAGES Floods Working Group that fosters collaborations. Sediment coring on Lake Bourget was performed using the French national sediment coring facility C2FN, in the framework of the excellence equipment project Equipe CLIMCOR (11-EQPX-0009, W.R., F.A., P.S. and B.W.) funded by the French National Agency for Research, ANR. The study of Lake Bourget sediment cores was performed in the framework of the CRIT-LAKES project funded by the Université Savoie Mont Blanc and the national CNRS programme EC2CO BIOHEFECT. The data analysis was performed in R using the supporting package trend. The authors acknowledge comments on preliminary publication versions from J.D. Creutin, G. Durand, C. Obled and M. Ménégoz as well as further colleagues for informal discussion during our Friday's beer.

Author contributions

All authors designed the study and B.W. wrote the first draft of the paper. B.W. collated the database with the help of B.A., W.R., M.C., C.G.-C., L.G., R.I., P.S., T.S. and S.B.W. W.R. conducted the sedimentological and geochronological analyses of the Lake Bourget sequence. B.W., M.N. and J.B. conducted the statistical analyses. All authors contributed to interpreting the results. All authors contributed to framing and revising the paper.

Competing interests

The authors declare no competing interests.

Additional information

Extended data is available for this paper at https://doi.org/10.1038/s41561-021-00878-y.

Correspondence and requests for materials should be addressed to B. Wilhelm.

Peer review information *Nature Geoscience* thanks Samuel Munoz and the other, anonymous, reviewer(s) for their contribution to the peer review of this work. Primary Handling Editor: James Super.

Reprints and permissions information is available at www.nature.com/reprints.

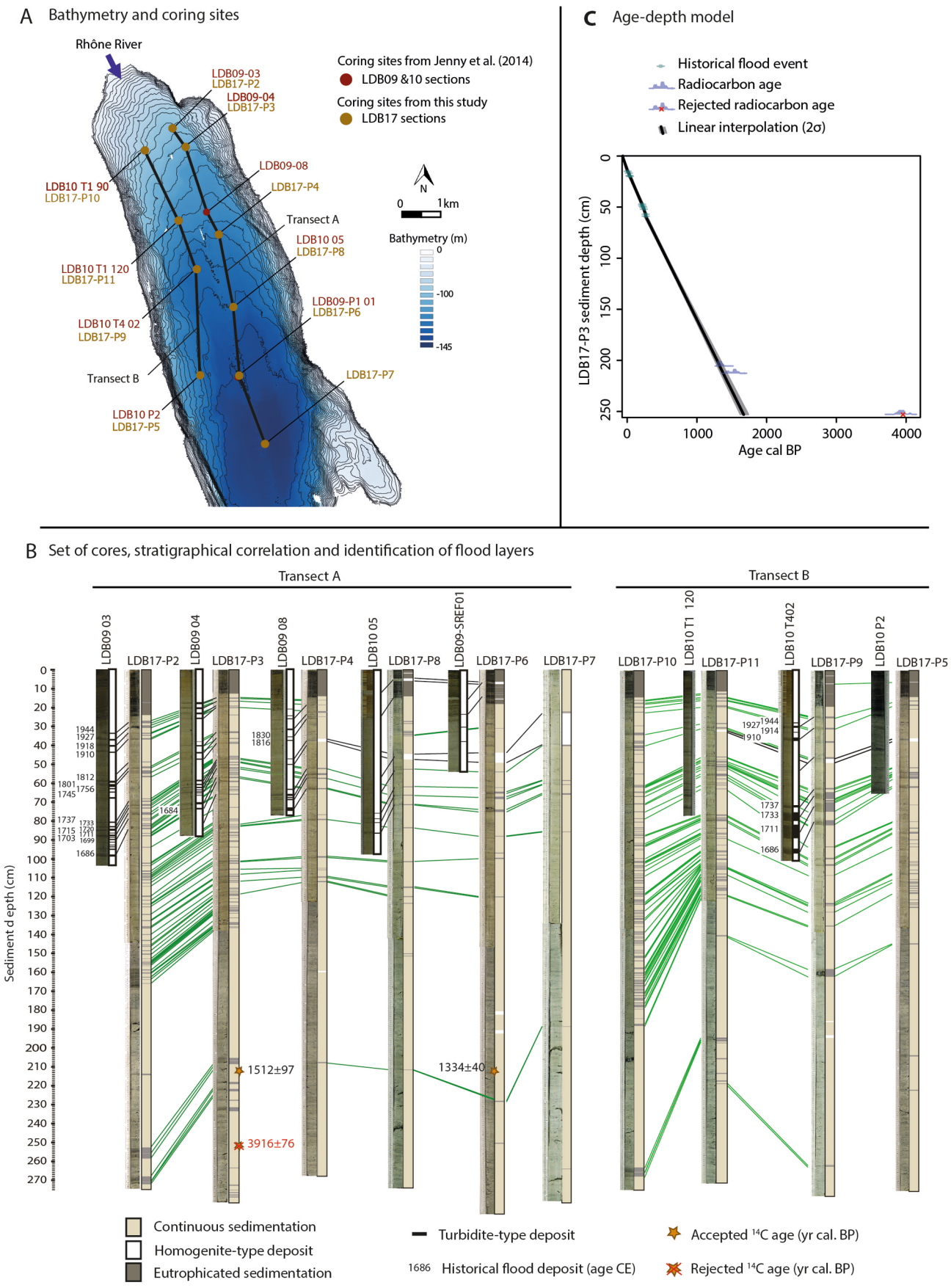

Extended Data Fig. 1 | See next page for caption.

Extended Data Fig. 1 | Data acquired to extend the 350-year paleoflood record of the Rhône River to the the last millennium. Data acquired to extend the 350-year paleoflood record of the Rhône River to the the last millennium. The method used is identical to Jenny et al. (2014)[56]. (A) Bathymetry of Lake Bourget and coring sites from Jenny et al. (2014)[56] and from the 2017 campaign (this study). (B) Stratigraphical correlation of the two core datasets along transect A and B, with indications of historical flood dates[56] and radiocarbon samples (Extended Data Table 4). (C) Age-depth model based on historical flood events and radiocarbon ages, using the software-package 'clam'[58].

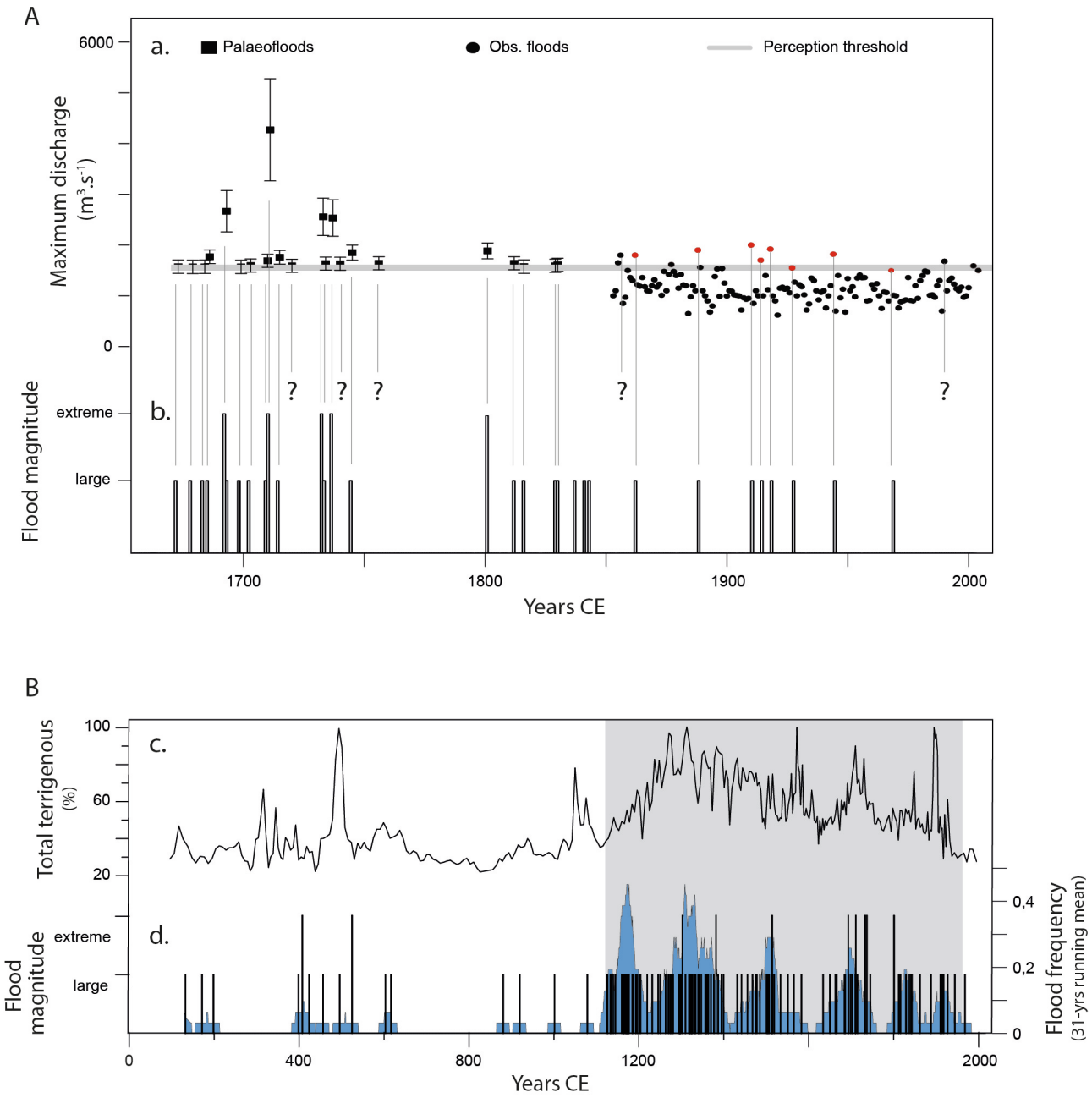

Extended Data Fig. 2 | Evaluation of the newly reconstructed Lake Bourget palaeoflood record. Evaluation of the newly reconstructed Lake Bourget palaeoflood record over the last 350 years (**a**) and the last two millennia (**b**). Over the last 350 years, the new record (b.) is compared to the record from Evin et al. (2019)[23](a.), which is an update of the dataset from Jenny et al. (2014)[56] that combined reconstructed palaeoflood discharges from 1650 to 1852 (black squares) and annual flood discharges from 2010 to 1852 (black and red dots). Red dots denote the floods recorded in the sedimentary sequence among the gauged, annual floods (black dots). Our new record includes 27 on these 32 floods and the five extreme floods correspond well to the largest flood discharges. The lacking floods in our dataset can be related to the lower number of sediment cores compared to Jenny et al. (2014)[56] and Evin et al. (2019)[23]. Over the last 2000 years, the new record (d) is compared to the record from Arnaud et al. (2016)[60], which correspond to detrital inputs brought by the Rhône River floods to the deepest part of Lake Bourget. These detrital inputs were very low in the oldest part of the record and largely increased during the Little Ice Age. This period of increased detrital inputs corresponds well to higher occurrence of flood events. Therefore, these comparisons support the robustness of our extended Rhône River palaeoflood record.

Extended Data Table 1 | List of the 33 existing palaeoflood records reconstructed from lake sediments in the European Alps. List of the 33 existing palaeoflood records reconstructed from lake sediments in the European Alps and selection of the 27 used in this study in bold, with information about location/coordinates, lake catchment characteristics as well as time length and characteristics of records. Abbreviations as follows: Lat. = latitude, Long. = longitude, Flood season: Sp = Spring, S = Summer, A = Autumn, W = Winter and U = Unknown, D = number of dating points (v = varved record), F = number of floods events recorded, M = Magnitude of floods reconstructed, C = Calibrated record and Ref. = reference. * = explanation for the record rejection from the study

	Lake	Short name	Lat.	Long.	Lake altitude (m a.s.l.)	Lake catchment area (km2)	Max. catchment altitude (m a.s.l.)	Flood season	Start year (CE)	End year (BP)	D	F	M	Ref.
1	**Allos**	ALO	44.23	6.72	2230	5	2672	A (S)	2009	1300	8	116	Yes	16
2	**Alzasca**	ALZ	46.26	8.59	1855	1	2292	S, A	2010	10000	10	567	No	17
3	**Ammersee**	AMM	48.00	11.12	533	709	2185	Sp, S	1999	5510	v	1501	No	18
4	**Anterne**	ANT	45.99	6.79	2063	2.5	2804	S	2007	10100	21	442	Yes	19
5	**Baldegg**	BAL	47.2	8.26	463	73	862	U	2002	10100	15	303	No	20
6	**Blanc Aig. Rouges**	BAR	45.98	6.92	2352	1	2695	S	1950	1300	8	158	Yes	21
7	**Blanc Belledonne**	BLB	45.18	5.97	2170	3	2978	S	2008	210	8	57	Yes	22
8	**Bourget**	LDB	45.77	5.84	231	4600	4810	A, W	2012	300	16	31	Yes	23
9	**Cadagno**	CAD	46.54	8.71	1921	2	2668	S	2009	12000	10	460	No	24
10	**di Braies**	BRA	46.69	12.08	1492	30	2810	S, A	2000	2900	v	60	No	25
11	**Faelen**	FAE	47.25	9.42	1446	5.1	2367	S, A	2009	9250	8	228	No	20
12	**Foréant**	FOR	44.71	6.99	2620	3	3210	S, A	2014	1050	9	139	Yes	26
13	**Garlate**	GAR	45.82	9.41	198	44	1035	S, A	2011	6500	11	465	No	17
14	**Glattalp**	GLA	46.92	8.9	1850	6.8	2717	S	2011	10400	7	564	No	20
15	**Grimsel**	GRI	46.57	8.33	1908	2	2966	S	1930	9300	8	86	No	20
16	**Hinterburg**	HIN	46.72	8.07	1514	1.6	2307	S, A	2010	8300	9	130	No	20
17	**Hinterer Schw.**	SCH	47.18	9.33	1159	5	2260	S, A	2009	11000	8	87	No	20
18	**Iffig**	IFF	46.39	7.41	2065	4.6	3246	S	2010	10100	15	158	No	20
19	**Inferiore di Laures**	INF	45.41	7.24	2450	7	3365	S, A	2013	200	12	60	No	27
20	**Lauerz**	LAU	47.04	8.61	447	69	1698	U	2004	1900	5	54	No	20
21	**Ledro**	LED	45.87	10.75	653	111	2047	S,A (Sp W)	2008	10500	18	861	No	28
22	**Mondsee**	MON	47.48	13.23	481	241	1782	S (Sp)	2005	7100	v	271	No	29
23	**Oeschinen**	OES	46.50	7.73	1580	20.4	3605	Sp, S	2010	1106	v	438	No	30
24	**Savine**	SAV	45.10	6.55	2447	3.5	3310	A (S)	2014	5630	11	200	Yes	31
25	**Seelisberg**	SEE	46.96	8.57	740	2.8	1923	S, A	2004	10700	11	234	No	20
26	**Trueb**	TRU	46.79	8.39	1766	6.2	3238	S	1920	2600	5	107	No	20
27	**Thun**	THU	46.69	7.71	558	1120	3683	S, A (Sp)	2007	100	3	15	No	32
28	Iseo	ISE	45.72	10.1	*Record strongly disturbed by human activities									33
29	Iseo	ISE	45.01	10.00	*Record strongly disturbed by human activities									34
30	Silvaplana	SIL	46.24	9.52	*Record not covering complete periods of interest									35
31	Gers	GER	46.02	6.72	*Record strongly disturbed by human activities									36
32	Ghirla	GHI	45.91	8.82	*Record not containing dates of flood occurrences over an entire period of interest									17
33	Muzelle	MUZ	44.95	6.08	*Record strongly disturbed by geomorphological changes									37

Extended Data Table 2 | AMS radiocarbon dates for the new Lake Bourget core dataset. AMS radiocarbon dates for the new Lake Bourget core dataset, measured at the Poznań radiocarbon laboratory, calibrated using the IntCal13 calibration curve[57]. The radiocarbon age in bold was rejected given its old age compared to other (radiocarbon and historical) dates (Extended Data Fig. 3)

Sample Name	Core	MCD (cm)	Radiocarbon age	Age cal. yr BP 2σ range	Age cal yr AD-BC 2σ range	Sample type
LDB17-1	LDB17-P6B	212.4	1430 ± 30	1334 ± 40	575-657 AD	wood
LDB17-2	LDB17-P3B	212.8	1635 ± 30	1512 ± 97	340-535 AD	wood
LDB17-3	**LDB17-P3B**	**252.8**	**3620 ± 35**	**3916 ± 76**	**2125-1890 BC**	**wood**

Extended Data Table 3 | List of the 27 selected palaeoflood records used in this study for the different analyses of flood occurrence and magnitude. List of the 27 selected palaeoflood records used in this study for the different analyses of flood occurrence and magnitude. A record is used for flood occurrence analyses when it fully covers the time period of interest or for flood magnitude analyses when it includes information about magnitude. When a record is used for flood occurrence analyses, a number is marked that corresponds to the mean flood return period of the record for the given period, that is the number of recorded flood events divided by the considered time length. When a record is used for flood magnitude analysis, a number is marked that corresponds to the site number (Nr.) used in Extended Data Table 1 and Fig. 3. The last 150 years cover 1850–2000 CE; the Industrial Era 1800–2000 CE; the Last Millennium 950–1850 CE and the Holocene 9000–1000 years BP

		For the analyses of flood occurrence				of flood magnitude
		Industrial Era	Last Millennium	Holocene	over the last 150 years	Last Millennium
Lake	Short name	Fig. 1 and 2	Fig. 1 and 2	Fig. 1 and 2	Fig. 2	Fig. 3
Allos	ALO	8	9		10	Yes (Nr. 1)
Alzasca	ALZ	8	10		8	
Ammersee	AMM	3	3		4	
Anterne	ANT	12	10		13	
Baldegg	BAL	15	12	53	14	
Blanc Aig. Rouges	BAR		7			Yes (Nr. 6)
Blanc Belledonne	BLB	5			5	
Bourget	LDB	13	9		50	Yes (Nr. 8)
Cadagno	CAD	14	27	22	17	
di Braies	BRA	20	39		19	
Faelen	FAL	11	25	45	10	
Foréant	FOR	5	7		5	Yes (Nr. 12)
Garlate	GAR	6	14		7	
Glattalp	GLA	13	16	19	11	
Grimsel	GRI			104		
Hinterburg	HIN	33	33		38	
Hinterer Schw.	SCH	29	35	163	38	
Iffig	IFF	13	21	118	11	
Inferiore di Laures	INF	5			4	
Lauerz	LAU	29	32		38	
Ledro	LED	3	4	14	4	
Mondsee	MON	14	13		14	
Oeschinen	OES	3	2		6	
Savine	SAV	13	20		10	Yes (Nr. 24)
Seelisberg	SEE	40	52	30		
Thun	THU				20	
Trueb	TRU		18			
Total number of records:		23	23	9	23	5
Mean flood return period:		14	18	63	15	

Extended Data Table 4 | List of collected temperature records from or close to the European Alps. List of collected temperature records from or close to the European Alps, sorted by time periods of interest, used in this study with information about site/location, archive type, proxy type, season and reference. Note that summer is the main flooding season (Table 1). References are the following: (1) Heiri O., Ilyashuk B., Millet L., Samartin S., Lotter A.F. (2015) Stacking of discontinuous regional palaeoclimate records: Chironomid-based summer temperatures from the Alpine region. The Holocene 25(1) 137–149; (2) Samartin S., Heiri O., Joos F., Renssen H., Franke J., Brönnimann S., Tinner W. (2017) Warm Mediterranean mid-Holocene summers inferred from fossil midge assemblages. Nature Geoscience. DOI: 10.1038/NGEO2891; (3) Büntgen U., Franck D.C., Nievergelt D., Esper J. (2006) Summer Temperature Variations in the European Alps, A.D. 755–2004, Journal of Climate, 19, 5606–5623; (4) Büntgen U., Tegel W., Nicolussi K., McCormick M., Frank D., Trouet V., Kaplan J.O., Herzig F., Heussner K.U., Wanner H., Luterbacher J., Esper J. (2011) 2500 Years of European Climate Variability and Human Susceptibility, Science 331, 578; (5) Corona C., Guiot J., Edouard J.L., Chalié F., Büntgen U., Nola P., Urbinati C. (2010) Millennium-long summer temperature variations in the European Alps as reconstructed from tree rings. Clim. Past, 6, 379–400; (6) Larocque-Tobler I., Heiri O., Wehrli M. (2010) Late Glacial and Holocene temperature changes at Egelsee, Switzerland, reconstructed using subfossil chironomids. J Palaeolimnology, 43:649–666; (7) Larocque-Tobler I., Stewart M.M., Quinlan R., Trachsel M., Kamenik C., Grosjean M. (2012) A last millennium temperature reconstruction using chironomids preserved in sediments of anoxic Seebergsee (Switzerland): consensus at local, regional and Central European scales. Quaternary Science Reviews 41, 49–56; (8) Mangini A., Spötl C., Verdes P. (2005) Reconstruction of temperature in the Central Alps during the past 2000 yr from a y18O stalagmite record. Earth and Planetary Science Letters 235, 741– 751; (9) Trachsel M., Kamenik C., Grosjean M., McCarroll S., Moberg A., Brázdil R., Büntgen U., Dobrovolný P., Esper J., Frank D.C., Friedrich M., Glaser R., Larocque-Tobler I., Nicolussi K., Riemann D. (2012) Multi-archive summer temperature reconstruction for the European Alps, AD 1053–1996. Quaternary Science Reviews 46 (2012) 66–79; (10) Auer I, Böhm R, Jurkovic A, Lipa W, Orlik A, Potzmann R, Schöner W, Ungersböck M, Matulla C, Briffa K, Jones PD, Efthymiadis D, Brunetti M, Nanni T, Maugeri M, Mercalli L, Mestre O, Moisselin J-M, Begert M, Müller-Westermeier G, Kveton V, Bochnicek O, Stastny P, Lapin M, Szalai S, Szentimrey T, Cegnar T, Dolinar M, Gajic-Capka M, Zaninovic K, Majstorovic Z, Nieplova E, 2007. HISTALP – Historical instrumental climatological surface time series of the greater Alpine region 1760–2003. International Journal of Climatology 27: 17–46

Period	Site, country	Archive	Proxy	Season	Ref.
Holocene	From multi sites, Alps, France and Switzerland	Lake sediments	Chironomids	Summer	1
	Gemini, northern Apennines, Italy	Lake sediments	Chironomids	Summer	2
	Verdarolo, northern Apennines, Italy	Lake sediments	Chironomids	Summer	2
Last Millennium	From multi sites, Alps, Switzerland	Tree rings	Wood density	Summer	3
	From multi sites, Alps, Austria	Tree rings	Ring width	Summer	4
	From multi sites, Alps, France, Switzerland and Italy	Tree rings	Ring width & wood density	Summer	5
	Egelsee, Alps, Switzerland	Lake sediments	Chironomids	Summer	6
	Seebergsee, Alps, Switzerland	Lake sediments	Chironomids	Summer	7
	Spannagel cave, Alps, Austria	Speleothem	Oxygen isotopes	Summer	8
	From multi sites, Alps, Switzerland and Austria	Multi	Multi	Summer	9
Industrial Era	Whole Alpine area	-	Instrumental data	Annual	10

Extended Data Table 5 | Changes in temperature by periods of interest from records of Extended Data Table 3. Changes in temperature by periods of interest from records of Extended Data Table 3. The Neoglacial Period (NP) covers 5000–1000 years BP; the Holocene Thermal Maximum (HTM) 9000–5000 cal. years BP; the Little Ice Age (LIA) 1450–1850 CE and the Medieval Climate Anomaly (MCA) 950–1250 CE. 19th c. = nineteenth century, 20th c. = twentieth century, Diff. = Differences in temperature between sub-periods and Ref. = Reference (see Extended Data Table 4)

		Temperature (°C)			
Period	**Site**	**NP**	**HTM**	**Diff. (°C)**	**Ref.**
Holocene	From multi sites, Alps, France and Switzerland	15.9	17.1	+1.2	1
	Gemini,northern Apennines, Italy	13.9	14.6	+0.7	2
	Verdarolo, northern Apennines, Italy	12.8	14.4	+1.6	2
	Median (±95% conf. Int.)			**+1.2 (±0.4)**	
	Site	**LIA**	**MCA**	**Diff. (°C)**	**Ref.**
Last Millennium	From multi sites, Alps, Switzerland	-1.6	-0.8	0.8	3
	From multi sites, Alps, Austria	-0.8	-0.3	0.5	4
	From multi sites, Alps, France, Switzerland and Italy	-1.2	-0.2	1.0	5
	Egelsee, Alps, Switzerland	-0.4	1.1	1.5	6
	Seebergsee, Alps, Switzerland	0.2	1.3	1.1	7
	Spannagel cave, Alps, Austria	0.9	1.9	1.0	8
	From multi sites, Alps, Switzerland and Austria	-0.5	-0.2	0.3	9
	Median (±95% conf. Int.)			**+1 (±0.4)**	
	Site	**19th c.**	**20th c.**	**Diff. (°C)**	**Ref.**
Industrial Era	Whole Alpine area	-0.5	-0.0	**+0.5**	10

Extended Data Table 6 | Sign and level of significance of relative changes in flood occurrence. Sign and level of significance of relative changes in flood occurrence obtained using the test of equal proportions as well as sign and level of significance of flood trends obtained respectively using a Poisson regression model with years as covariate and a Chi-square test. Si = sign of the change/trend; - = negative change/trend; + = positive change/trend; S=Level of significance; *** = p < 0.001; ** = p < 0.01; ** = p < 0.1; NA = no result due to the shortness of the record in relation to the studied period (Extended Data Table 2); NA* = no result due to a too limited number of recorded events in relation to the studied period

	Relative change in flood occurrence (Fig. 1)						Trends in the occurrence of large floods (Fig. 2)											
	Industrial Era		Last Millennium		Holocene		Industrial Era		Last Millennium		Holocene		1950-2000 CE		1900-2000 CE		1850-2000 CE	
	Si	S	Si	S	Si	S	Si	S	Si	S	Si	S	Si	S	Si	S	Si	S
ALO	-	*	-	***	NA		-	***	-	**			-		+		-	***
ALZ	NA*		+		NA		+		-				-	*	-		-	
AMM	+		-	***	NA		-	*	-	***			-		-	*	+	
ANT	-		-	**	NA		-	***	-	***			+	***	+	***	+	
BAL	-		-		-	***	-		-		-	***	NA*		+		-	***
BAR	NA		-		NA		NA		+	*			NA		NA		NA	
BLB	+		NA		NA		-		NA				-		-	***	+	
LDB	-		-		NA		-	***	+	*			+		-	***	+	
CAD	-	**	-	**	-	***	-	***	-	***	-	***	NA*		NA*		-	***
BRA	+		+		NA		+	**	-				-	*	+		+	
FAL	-		-	*	-	***	+	*	-	***	-	***	+		+	***	-	
FOR	-		-	**	NA		-		-	***			+		+		+	
GAR	-		-		NA		+		-	***			-	***	+		+	***
GLA	+	*	-		+		+	***	-		+	***	+		+	***	+	***
GRI	NA		NA		-		NA		NA		-	***	NA		NA		NA	
HIN	+		-		NA		+	***	-	***			NA*		+		+	
SCH	-		-	*	-	***	-	*	-	***	-	***	NA*		-		-	***
IFF	-		-		-	*	-	*	+		-	***	NA*		-	**	-	***
INF	-		NA		NA		-		NA				+		+	*	-	***
LAU	-		-	*	NA		-	*	-	***			NA*		NA*		-	
LED	-	**	-	**	-	***	-	***	-	***	-	***	-	*	-	*	-	***
MON	+		+		NA		+	**	+	**			+	*	+	*	+	***
OES	-	***	-	***	NA		-	***	-	***			+	***	+		-	***
SAV	+		-	***	NA		-	**	-	***			+		-		+	
SEE	-		-		-		-	***	-	***	-	***	NA		NA		NA	
THU	NA		NA		NA		NA		NA				NA*		-	*	-	***
TRU	NA		-	*	NA		NA		-	***			NA		NA		NA	
Total number of values	23	5	23	12	9	6	23	17	23	18	9	9	23	7	23	11	23	12

Extended Data Table 7 | Modified Mann-Kendall test of significance of warming/cooling trend. Modified Mann-Kendall test of significance of warming/cooling trend during the Holocene (9000–1000 BP), the Last Millennium (950–1850 CE), the Industrial Era (1800–2000 CE) and subperiods of the Industrial Era. Level of significance: *** = p < 0.001; ** = p < 0.01; ** = p < 0.1. Ref. = Reference (see Extended Data Table 4)

Period	Site	Time period	Significant warming/cooling trend	Ref.
Holocene (H)	From multi sites, Alps, France and Switzerland	9000-1000 BP	cooling **	1
	Gemini,northern Apennines, Italy	9000-1000 BP	cooling ***	2
	Verdarolo, northern Apennines, Italy	9000-1000 BP	cooling ***	2
	Site			**Ref.**
Last millennium (LM)	From multi sites, Alps, Switzerland	950-1850 CE	cooling **	3
	From multi sites, Alps, Austria	950-1850 CE	cooling ***	4
	From multi sites, Alps, France, Switzerland…	950-1850 CE	cooling *	5
	Egelsee, Alps, Switzerland	950-1850 CE	cooling	6
	Seebergsee, Alps, Switzerland	950-1850 CE	cooling *	7
	Spannagel cave, Alps, Austria	950-1850 CE	cooling ***	8
	From multi sites, Alps, Switzerland and Austria	950-1850 CE	cooling *	9
	Site			**Ref.**
Industrial Era (IE)	Whole Alpine area	1800-2000 CE	warming ***	10
	Whole Alpine area	1850-2000 CE	warming ***	10
	Whole Alpine area	1900-2000 CE	warming ***	10
	Whole Alpine area	1950-2000 CE	warming ***	10